Article

Not peer-reviewed version

Effect of Cetyl Pyridinium Chloride on Corrosion Inhibition Properties of Mild Steel in Acidic Medium

Chandradip Kumar Yadav , Shova Neupane , Benadict Rakesh , Amar Prasad Yadav , Tulasi Prasad Niraula , Ajaya Bhattarai *

Posted Date: 30 April 2024

doi: 10.20944/preprints202404.1187.v2

Keywords: FTIR; FESEM; EDX; inhibitor; mild steel; cetyl pyridinium chloride

Article

Effect of Cetyl Pyridinium Chloride on Corrosion Inhibition of Mild Steel in Acidic Medium

Chandradip Kumar Yadav [1, 2], Shova Neupane [2], Benadict Rakesh [3], Manoj Kumar Adhikari [1], Amar Prasad Yadav [1], Tulasi Prasad Niraula [4] and Ajaya Bhattarai [4]*

[1] Central Department of Chemistry, Tribhuvan University, Kirtipur, Nepal
[2] CSIR – Institute of Minerals and Materials Technology, Bhubaneswar-751013, India
[3] Mahendra Morang Multiple Campus, Biratnagar, Nepal
* Correspondence: Department of Chemistry, Mahendra Morang Adarsh Multiple Campus, Tribhuvan University, Biratnagar, Nepal. E-mail address: ajaya.bhattarai@mmamc.tu.edu.np (A. Bhattarai.).

Abstract: The corrosion inhibition behavior of cetyl pyridinium chloride (CPC) on mild steel (MS) in 0.5 M H_2SO_4 solution was examined using the weight loss method and potentiodynamic polarization method. The experimented MS surface was characterized by Fourier Transform Infrared Spectroscopy (FTIR), Field Emission Scanning Electron Microscopy (FESEM), and Atomic Force Microscopy (AFM). Corrosion rate and corrosion efficiency was calsulated via weight loss and potentiodynamic polarization methods where the corrosion rate in 0.5 M H_2SO_4 , 0.000192 M, and 0.0077 M of CPC solution was 12.09×10^{-3}, 8.23×10^{-3}, 6.63×10^{-5} (mm/Year), respectively and the inhibition efficiency of 94.42% and 98.54%. FESEM studies demonstrated the corrosion attack on MS surface. Also, the EDX showed the presence of nitrogen of CPC. Thus, CPC acts as an important corrosion inhibitor.

Keywords: : FTIR; FESEM; EDX; inhibitor; mild steel; cetyl pyridinium chloride

1. Introduction

Mild steel is widely used in the building, transportation, and maritime industries due to its high mechanical and thermal stability, low cost, and availability. However, mild steel is prone to rust, especially in marine environments [1]. A fundamental, scholarly, and industrial problem that has received a lot of attention recently is mild steel corrosion. Many methods have been employed to prevent steel from corrosion, including electroplating, thermal spraying, micro-arc oxidation, and the application of organic coatings [2]. One of the most practical and affordable ways to prevent corrosion on metallic surfaces in very acidic environments is to use inhibitors [3].Organic coatings are the one of the researched methods of controlling the corrosion. Adsorption of organic molecules isolates the steel substrate from corrosive media, offering long-lasting protection. However, during the curing process, the solvent evaporation of pure organic adsorption might give rise to micropores, which inevitably affects the adsorption's barrier qualities[4].

In a variety of sectors, pickling steel at temperatures as high as 60°C is a common usage for mineral acids. This technique is effective not only at cleaning industrial equipment but also at acidizing oil wells and eliminating corrosion scales from steel surfaces without completely destroying the metal [4].

The most potent pickling inhibitors are organic compounds containing hetero atoms, such as oxygen, phosphorus, nitrogen, sulfur, and many linkages or aromatic rings. The amount of loosely bound p-electrons and lone pairs of electrons in these functional groups are important structural elements that affect these compounds' inhibitory effect. These compounds reduce the amount of active corrosion sites on the metal surface by adsorption, protective layer deposition, or the creation of an insoluble mixture[5].

Unfortunately, the majority of organic compounds used as corrosion inhibitors are dangerous to humans and the environment, thus safer, more environmentally friendly alternatives must be used

 doi:10.20944/preprints202404.1187.v2

in their place. In this regard, the prime focus of current research trends is the search of ecologically benign, cost-effective, and non-toxic green chemicals for corrosion inhibition. Among many well-reported compounds, amino acids have been used as biodegradable, non-toxic, and low-cost corrosion inhibitors[6]. It has been discovered that the sulfur-containing amino acid L-methionine is a potent corrosion inhibito [7]r. Using Tafel polarization measurements, nineteen naturally occurring amino acids including methionine - were examined for their ability to suppress the corrosion of mild steel in H_2SO_4[8,9]. Based on available data, organic inhibitors function through adsorption and create a protective coating around the metal. Corrosion can be effectively inhibited by organic compounds like CPC, which include heteroatoms with high electron density, such as phosphorus, sulfur, nitrogen, and oxygen, or by compounding numerous bonds that act as adsorption centers [10].

Among the inhibitors that work well in acidic solutions are those that contain nitrogen, such as mercapto functional compounds and derivatives of amines like pyridazine, quinoline, and pyridine, as well as pyrazole, pyrazine, acridine, benzimidazole, and triazole. The majority of these compounds have demonstrated mixed-type corrosion inhibition in acidic solutions, protecting mild steel. Benzothiazoles have been employed as corrosion inhibitors for copper and steel[11].

Surface analytical approaches are needed to characterize corrosion inhibitor films to have a comprehensive understanding of the adsorption mechanism for corrosion inhibitors. According to (Mobin et al., 2017) weight loss and potentiodynamic measurement complemented by FTIR, and EDX have proven to be effective methods for examining corrosion processes and inhibitor performance.

The capacity of surfactant molecules to assemble at surfaces and in solution is associated to their ability to suppress corrosion. Based on the surfactant inhibitor's micellar characteristics in a given media, its efficiency has been investigated. In a variety of applications, surfactants have demonstrated encouraging performance as corrosion inhibitors for metals and alloys.[13].

Depending on the surfactant concentration, the adsorbed molecules form a monolayer, bilayer, or micelle hemimicelles, which lessen corrosion attacks by preventing acid from attacking the surface. To increase the effectiveness of organic molecules as inhibitors, the surfactant can be employed either by itself or in combination with them [14]. Acids and surfactants are likely to interact to create complex structures that aid in adhesion to the surface and provide increased corrosion resistance[15].

The goal of this study is to learn more about how CPC inhibits corrosion on mild steel in a 0.5 M H_2SO_4 solution. Weight loss and potentiodynamic polarization methods were used to calculate the inhibition efficiency and FTIR, FESEM, EDX, and AFM were the characterization techniques used in the present study.

2. Materials and Method

2.1. Materials

The mild steel used in corrosion inhibition studies had the following composition (wt%): 0.20 C, 0.53 Mn, 0.036 Si, 0.11 S, 0.098 P, and Fe for the remainder. The samples, which measured 15.92, 13.38, and 1.31 mm, were press-cut from mild steel sheets, machined, and abraded with emery sheets. This was followed by a rinse with acetone and double distilled water before air drying and directly used for the measurements. The inhibitor CPC (molecular mass: 358 g/mol) was used exactly as received. A stock solution of 0.00192M and 0.0077M CPC was prepared in 0.5 M H_2SO_4 (AR grade). All solutions were prepared using double-distilled water. The weight loss experiment was carried out at 25°C. Figure 1 shows the molecular structure of the CPC.

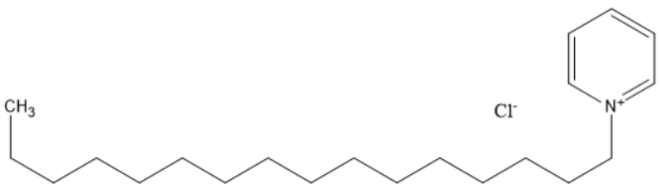

Figure 1. cetyl pyridinium chloride(CPC).

 doi:10.20944/preprints202404.1187.v2

2.2. Methods

2.2.1. Weight Loss Measurements

The recently built mild steel specimens were suspended in 50 mL beakers containing 25 mL of test solution and maintained at 25°C in a thermostated water bath equipped with glass rods and hooks. The weight loss was computed by subtracting the specimens' original weight from their weight at a specific moment in time[8]. Both the uncontrolled solution and the solution containing CPC surfactant mixes were subjected to the measurements.

Weight loss experimentation took six hours. The average corrosion rate was determined after the specimens were dipped three times. Less than 5% separated the three identical measurements from one another. The following formula was used to determine the corrosion rates.

$$\text{Corrosion Rate (CR)} = \frac{Weight\ loss\ (W)}{Area\ (A) \times Time(T) \times Density(d)} \times 8.76 \times 10^{4}$$

Where W is the weight loss of the MS (g) after immersion time, t (hours), A is the MS's area (cm^2), and d is the MS's density ($g\ cm^{-3}$).

$$\textbf{Inhibition Efficiency } (IE)\ \% = \left(W_o - W_i / W_o\right)\ \text{X } 100$$

Where W_o is the MS weight loss in the absence of an inhibitor and W_i is the MS weight loss in the presence of an inhibitor.

$$\text{Inhibition Efficiency (IE) \%} = (W_o - W_i / W_o)\ \text{X } 100$$

Where W_o is the MS weight loss in the absence of an inhibitor and W_i is the MS weight loss in the presence of an inhibitor.

2.2.2. Potentiodynamic Polarization Measurements:

Three electrode systems were used for potentiodynamic polarization measurements, and each device was Gamry controlled by a PC running AUTOLAB's general-purpose electrochemical system (GPES) software. The experiments were conducted using. The working electrode is a mild steel sample, the counter electrode is platinum wire, and the reference electrode is a saturated calomel electrode (SCE+ 0.241V)[18].

Potentiodynamic polarization was recorded from -0.3 V to +0.3 V vs. OCP at a scan rate of 0.5 mV/s, examining the potential from cathodic to anodic limits. greater energy than the constant open circuit voltage[16]. All measurements were conducted at room temperature, 25°C. Before starting the measurements, the specimen was submerged in the solution for thirty minutes to create a steady state, as shown by a constant potential. From the measured Icorr values, the IE was calculated using the following relationship[17].

$$Corrosion\ inihibition\ efficency\ = \frac{I_{Corr} - I^{*}_{Corr}}{I_{Corr}} \times 100\ \%$$

where I^{*}_{corr} = corrosion current when an inhibitor is present, and I_{corr} = corrosion current when an inhibitor is not present.

2.2.3. Characterization Techniques

In the investigation of the corrosion protection behavior of mild steel in 0.5 M H_2SO_4, the mild steel samples were immersed in a 0.5 M acidic solution for 6 hours, both in surfactant solution without surfactant. To scrutinize the mild steel surface, FTIR, FESEM, EDX, and AFM techniques were utilized.

The surface morphology of the steel sample that has corroded both with and without the inhibitors was studied using FTIR (Model no: Bruker company limited, America), FESEM (model: JSM IT800, JEOL Field emission scanning electron microscopy, Made in Japan), EDX (Model no: Elect Super Company EDAX, Made in America) and AFM (model: Jp 02069 JPK Nanowizard, Bruker). The surface morphology of mild steel was studied by looking for surface imperfections, such as pits or

 doi:10.20944/preprints202404.1187.v2

obvious abnormalities like cracks, under an optical microscope before any corrosion response began. Solely the specimens possessing a smooth, pit-free surface were submerged. The samples were submerged in 0.0077 M CPC of 0.5 M H_2SO_4 at 25^0 C for 6 hours. Following the test, the specimens underwent a comprehensive cleaning process in double-distilled water, followed by drying and examination with an FTIR, FESEM, EDX.

3. Results and Discussion

3.1. Weight Loss Measurements

The corrosion behavior of mild steel in 0.5 M H_2SO_4 with and without varying CPC concentrations was investigated at 25°C using a weight loss approach. Table 1 presents the results of the 6-hour immersion. With the temperature at 25°C and the inhibitor concentration, CPC reduces the rate of mild steel corrosion proportionately when compared to a free acid solution[4].

The IE increases with rising CPC concentrations. As inhibitor concentration rise, more CPC molecules are adsorbed on the steel surface at higher concentration because of the increased IE, which enhances surface coverage and results in the formation of a protective layer. The relatively low IE at lower CPC concentrations may be due to the solubility of adsorbed intermediates generated on the surface as well as the limited surface coverage brought on by the tiny molecular area[19].

At 25°C, individual tests of mild steel corrosion in 0.5 M H_2SO_4 with and without different CPC concentrations were conducted to examine the impact of CPC on its corrosion-inhibitory behavior. The results are presented in Table 1.

Table 1. Corrosion rate and inhibition efficiency of CPC using weight loss method.

S.N.	Concentration	Corrosion Rate (mm/Year)	% of Inhibition efficiency
1.	0.5 M H_2SO_4	12.09×10^{-3}	-
2.	0.00192M CPC	8.23×10^{-3}	99.66
3.	0.0077 M CPC	6.63×10^{-5}	99.99

It has been found that IE is more affected by higher surfactant concentrations. The kind and concentration of surfactant molecules determine how they adsorb on surfaces.

Although the adsorption of cationic surfactants on like-charged surfaces is less well understood, hydrogen bonding or attractive dispersion forces may play a role, just like in the case of nonionic surfactants. At low surfactant concentrations, the adsorption behavior is typically explained by a simple electrical double-layer model [12].

Catalytic surfactant monomers adsorb as separate ions apart from each other. Tail-tail interactions may cause head groups to face the surface at higher concentrations of adsorbed surfactants. Surfactant monomer head groups form a bilayer on the surface, with one faceting the surface and the other the bulk liquid [20]. The surfactant molecules' adsorption on the steel surface slows down the corrosion process by lowering the quantity of electrons accessible for reactions. Micelle-like aggregates spontaneously form at far lower concentrations than bulk CMC, and cationic surfactants adsorb to surfaces with opposing charges to form a complete bilayer [21]. The corrosion rate of acid and CPC at concentrations 0.05 M acid (H_2SO_4), 0.000192 M, and of 0.0077 M of CPC was calculated at $12.09\times10^{-3,}$ $8.23\times10^{-3,}$ 6.63×10^{-5} (mm/Year) respectively.

3.2. Potentiodynamic Polarization Measurement

A potentiodynamic polarization study of a surfactant on mild steel employs electrochemical methods to explore how the presence of the surfactant influences the corrosion tendencies of mild steel. This investigation typically entails immersing mild steel samples in an electrolyte solution containing the surfactant and subjecting them to controlled changes in electrode potential while monitoring resulting currents [22]. Through analyzing parameters such as corrosion potential, corrosion current density, and polarization resistance, researchers gain insights into how the surfactant either inhibits or exacerbates corrosion processes on the mild steel surface. Such studies

 doi:10.20944/preprints202404.1187.v2

are crucial for understanding the effectiveness of surfactants in protecting mild steel against corrosion, informing potential industrial applications where mild steel components are exposed to corrosive environments [23].

Using the potentiodynamic polarization methodology, the Tafel polarization approach calculated the corrosion protection potential of CPC as a function of inhibitor concentration and immersion time in a corrosive solution. A thorough description of the results is provided below. The concentration of the inhibitor and length of immersion determine CPC in a corrosive solution[24]. Figure 2 depicts the Tafel polarization behavior of a mild steel electrode immersed in a 0.5 M H_2SO_4 solution blank and exposed to 0.00192 M and 0.0077 M CPC concentrations[25].

The shape of the anodic and cathodic Tafel slopes provides information on the processes (reactions) taking place on the surface of the mild steel electrode. At the cathodic site, where cathodic currents are produced, electrons released from the breakdown of Fe atoms into Fe^{2+} ions transform H^+ ions into H_2 gas, which is the main source of anodic currents [26]. Figure 2 illustrates how the formation of stable corrosive compounds (such as $FeCl_2$) is implied by the falling slope of anodic branch and comparatively steady current response following around 160 mV of overpotential at the anodic site [27].

Cathodic currents are created at the cathodic site when H+ ions are transformed into H_2 gas. The anodic branch slope in Figure 2 decreases following approximately 160 mV of overpotential at the anodic site, signifying the generation of stable corrosive chemicals (such as $FeCl_2$) [28].

The current response then becomes rather steady. The inhibitory efficiency (IE) of CPC at each concentration was determined using Tafel polarization data, and the findings are shown in Table 2. As CPC concentrations rise from 0.00192 M to 0.0077 M, Figure 2 shows how cathodic and anodic current densities decrease and stable corrosive products (such as $FeCl_2$) form[29].

The anodic current was almost equally reduced by both CPC concentrations, while the cathodic zone shows a stronger tendency [30]. The greatest IE (98.54%) was reached with a CPC concentration of 0.0077 M and an i_{corr} of 0.00025Acm^{-2}. The following formula is used to get IE: Since the effects of the two dosages on anodic sites are almost comparable, the mechanism of concentration-dependent anodic CPC inhibition is most likely at play.

Cl ions may be preferentially adsorbed at anodic sites due to electrostatic contact, covering reactive (anodic) sites, at CPC concentrations of 0.00192 M and 0.0077 M, respectively. Furthermore, the lower values of a (Table 2) show that the rate of increase in anodic current density is noticeably slower in the presence of both inhibitor dosages than in the absence of them due to the slow rate of Fe dissolution [31].

As concentration increases, anomalous current responses are observed at the cathodic site, where CPC molecules attempt to arrange themselves into different geometrical groups inside the adsorbed layer. Lower CPC concentrations of 0.00192 M appear less effective than higher concentrations, with an IE value of 94.42%. Under the same circumstances, the structure and coatings produce higher IE values in 0.0077 M CPC. At a CPC concentration of 0.0077 M, the adsorbed surfactant layer was stable on the mild steel surface.

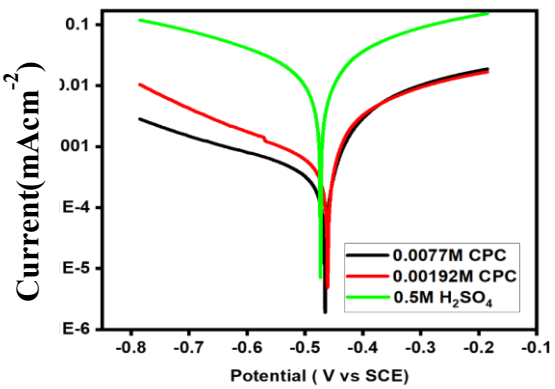

 doi:10.20944/preprints202404.1187.v2

Figure 2. Potentiodynamic curves for mild steel in 0.5 M H_2SO_4 in the absence of and presence of 0.00192 M ,and 0.0077 M concentrations of CPC.

Table 2. Corrosion rate and inhibition efficiency of CPC using the Potentiodynamic polarization method.

S.N.	Concentration	Corrosion Current (Acm^{-2})	% of Inhibition efficiency
1.	0.5 M H_2SO_4	17.21×10^{-3}	-
2.	0.00192 M CPC	0.96×10^{-3}	94.42
3.	0.0077 M CPC	0.25×10^{-3}	98.54

The discovered differences in E_{corr} and I_{corr} between samples shed light on the adsorption's corrosion processes. The evolution of E_{corr} values in surfactant-containing samples points to a significant reliance on CPC levels in the CPC-Fe layer. The best balance in this composition of the sample is shown by the sample CPC's peak performance, which shows the highest positive E_{corr} and the lowest I_{corr}. Additionally, it is shown that samples with higher CPC concentrations have the best corrosion inhibition capabilities.

The sample with the lowest corrosion inhibition characteristics is the one with a lower concentration of CPC. There appears to be a correlation between the molecule's adsorption on mild steel and the thickness of the surfactant layer; samples with lower surfactant concentrations have thinner mild steel layers. It correlates with the strongest corrosion inhibition qualities at greater surfactant concentrations [32].

3.3. Fourier Transform Infrared Spectroscopy (FTIR) Analysis

FTIR is a technique for determining the functional groups in a sample by analyzing infrared light absorption. It has to do with CPC precipitation, and the infrared spectra of the precipitate are typically used to identify the functional groups [33]. Moreover, using FTIR technology, the Functional Group Identification technique assessed CPC adsorption as a function of inhibitor concentration and immersion time in corrosive solutions [34].

A thorough description of the results is provided below. Figure 3 illustrates the adsorption behavior of a mild steel electrode immersed in a 0.5 M H_2SO_4 solution blank and exposed to CPC concentration (0.0077 M). The mild steel functional group provides information on the adsorption process occurring on the surface of the electrode. Figure 3b shows the functional group of the CPC molecule. Figures 3a,c, respectively, depict the mild steel functional groups prior to and following immersion in a CPC solution. When CPC molecules come into contact with mild steel, adsorption takes place [35].

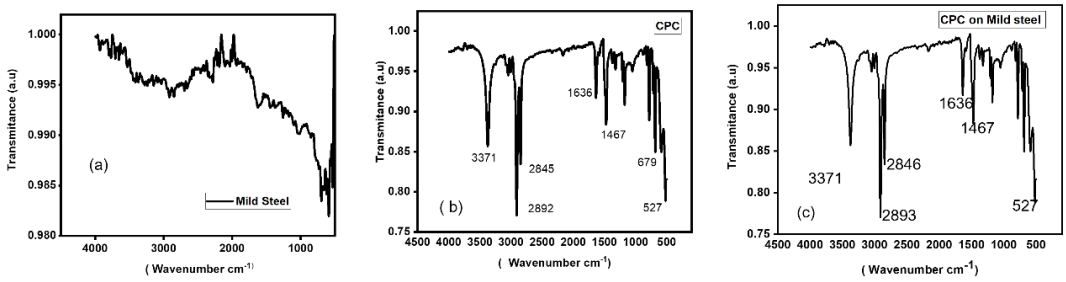

Figure 3. Fourier Transform Infrared Spectroscopy (FTIR) of Mild steel, CPC, and CPC adsorbed on mild steel.

Functional Groups in CPC: Pyridinium group (which have a positive charge on nitrogen atoms) found in cetylpyridinium chloride. Additional functional group from the interacting chemicals may be present in the precipitate [36]. Aromatic: Usually observed between 1342 and 1266 cm^{-1} (C-N

 doi:10.20944/preprints202404.1187.v2

stretching). Aromatic: Usually detectable between 1690 and 1640 cm^{-1} (C=N stretching). It is common to detect aliphatic C-H stretching in the range of 3000-2500 cm^{-1}. It is common to see aromatic C-H stretching in the range of 2000-1650 cm^{-1}. The C-H stretching vibrations of the alkyl chain are observable in the 2800-3000 cm^{-1} range. This explains why mild steel submerged in CPC solution corrodes at a low pace, which is further corroborated by electrochemical tests.

3.4. FESEM-EDX Studies

Figure 4a,b) shows the FESEM image in the absence and presence of 0.0077M CPC in 0.5 M H_2SO_4 [37].

The MS surface corrodes far less in the presence of inhibitors (CPC) than in 0.5 M H_2SO_4 solution, as seen in Figure 4b [38].

The surface morphology reveals the protection of MS surface by the presence of CPC molecules in the acid solution. The surface is more smooth compared to that in only acid solution.

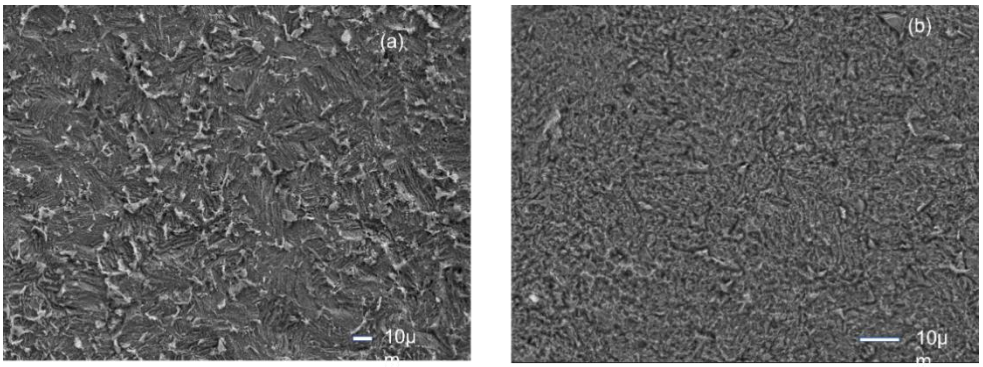

Figure 4. FESEM photomicrograph of the surface of mild steel after immersion for 6 h at 25 °C in (**a**) 0.5 M H_2SO_4 and (**b**) 0.0077 M CPC inhibited in 0.5 M H_2SO_4 solution.

The surface composition was determined by EDX analysis. which indicated the presence of Nitrogen peak of the cetyl pyridinium chloride,.

This illustrates the inhibitory effect of cetyl pyridinium chloride, which forms a layer on mild steel to protect the corrosion.

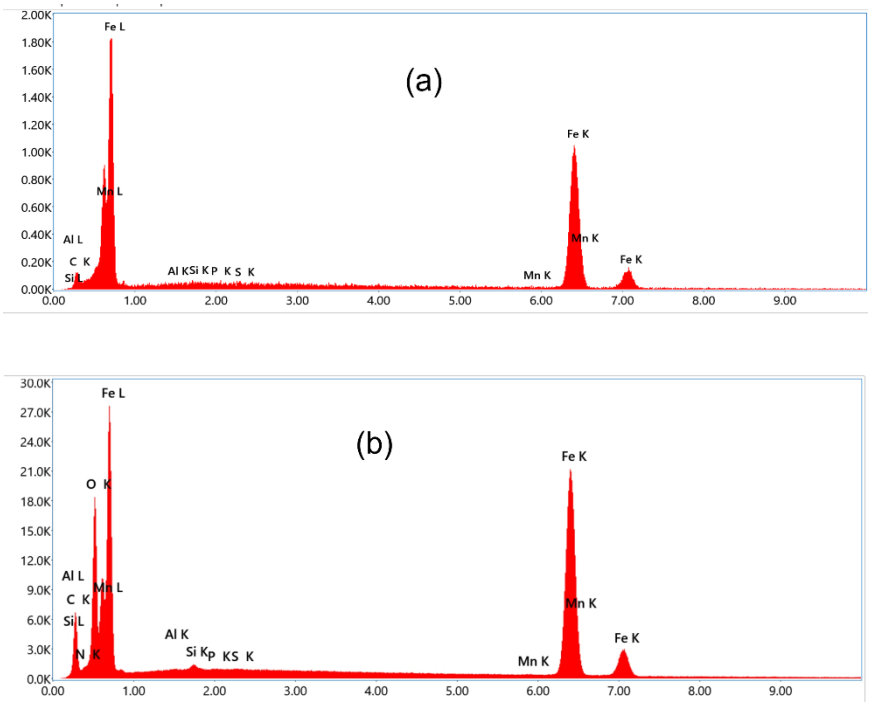

 doi:10.20944/preprints202404.1187.v2

Figure 5. EDX data of mild steel after immersion for 6 h at 25 °C. 0.5M in (**a**) 0.5 M H_2SO_4, (**b**) 0.0077 M CPC inhibited in H_2SO_4 solution.

3.5. Atomic Force Microscopy (AFM) Study

The morphologies of mild steel specimens with and without CPC after immersion in 0.5 M H_2SO_4 solutions for 6 h at 25 °C are shown in Figure. 6. Because of the corrosion attack, the surface showed a very uneven topography when the inhibitor was absent (Figure 6a). The average roughness (Ra) of mild steel in 0.5 M H_2SO_4 solution without inhibitor was found to be 4.4 nm using atomic force microscopy (Figure 6a)[39–41]. This roughness value is typical for the MS surface polished with SiC paper of 2000 grit size. A protective inhibitor layer formed on the mild steel surface when CPC was present, reducing corrosion damage and producing a surface with a Ra value of 108 nm (Figures. b and c). This higher roughness value is due to the presence of large molecular size CPC on the MS surface. Without an inhibitor, it is clear that the mild steel surface was extensively corroded with regions of uniform corrosion (Figure 6a) [42]. Inhibitors, on the other hand, caused the specimen surface to become smoother (Figure 6b) . after immersion in 0.0077 M CPC The inhibitory effect of CPC by binding with the reaction sites on the MS surface is obvious, hence limiting the amount of interaction between the MS and the aggressive medium.

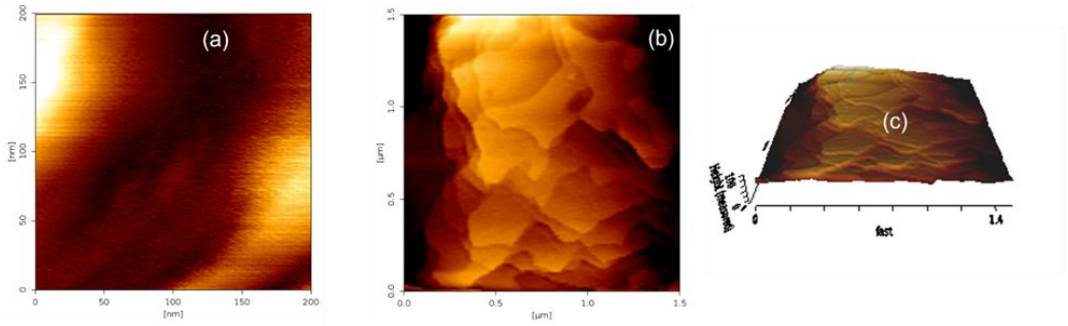

Figure 6. (**a**) AFM photograph of the surface of mild steel after immersion in 0.5 M H_2SO_4 for 6 h at 25 °C (**b**) The morphologies of mild steel specimens with 0.0077 M CPC after immersion in 0.5 M H_2SO_4 solutions for 6 h at 25 °C (**c**) 3D image of mild steel specimens with 0.0077 M CPC after immersion in 0.5 M H_2SO_4 solutions for 6 h at 25 °C presence of CPC.

3.6. Mechanism of CPC – Mild Steel

The interaction between the CPC's pyridinium functional group and the corroding steel surface is conceivable. Protonated pyridinium's functional group is adsorbed at anodic sites to prevent iron dissolution and at cathodic sites to halt the hydrogen evolution reaction [43–46]. This implies that the anodic and cathodic partial responses are regulated by the CPC through a multimodal inhibitory mechanism [46–53]. The fact that the CPC molecules adhere to the mild steel surface implies that, depending on their concentration, they self-aggregate there to form a variety of stripes that are uniformly wide, regularly spaced, and well-organized.[54–57]. The surface is adequately covered by the molecules' long-range interactions which is shown in Figures 7c and 8, which lowers the rate of corrosion.

 doi:10.20944/preprints202404.1187.v2

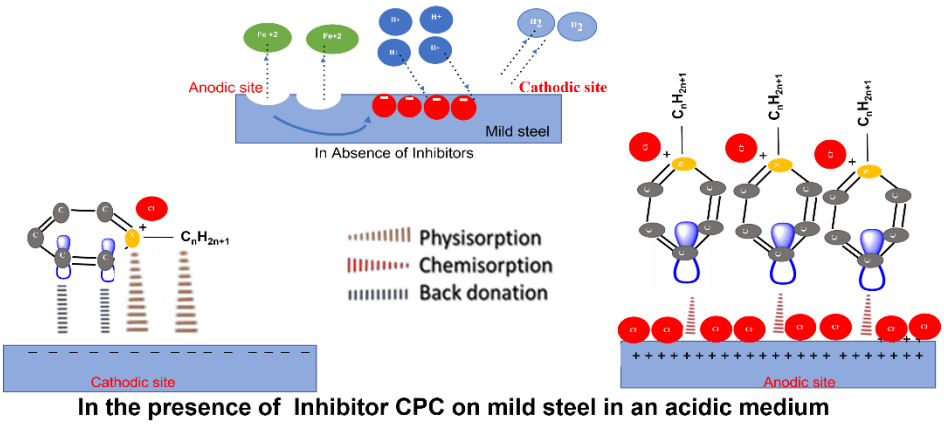

Figure 8.): Mechanism of CPC – Mild steel.

4. Conclusion:

Based on the results, it is concluded that the CPC demonstrated good mild steel corrosion inhibitor performance in 0.5 M H_2SO_4. The corrosion rate in 0.5 M H_2SO_4,0.000192 M, and of 0.0077 M of CPC in acid solution was calculated as 12.09×10^{-3}, 8.23×10^{-3}, 6.63×10^{-3} (mm/Year), respectively by weight loss method. The inhibition efficiency of CPC in two different concentrations 0.00192 M and 0.0077 M of CPC has been calculated at 94.42% and 98.54%, respectively by the potentiodynamic polarization method. FTIR measurement provides a comprehensive understanding of CPC adsorption on mild steel. FESEM and EDX studies demonstrated the reduced degradation of mild steel by CPC molecules. The corrosion attack on the surface of mild steel showed a very uneven topography in the absence of CPC.

Author Contributions: Credit authorship contribution statement. Chandradip Kumar Yadav: conceptualization, data curation, Investigation, Tulasi Prasad Niraula Shova Neupane, Benadict Rakesh: Methodology, Project administration. Amar Prasad Yadav, Ajaya Bhattarai: Formal analysis, Resources, Software, Funding acquisition, Validation, Visualization, Writing-review & editing.

Declaration of Competing Interest: The authors declare that they have no known competing financial interests or personal relationships that could have appeared to influence the work reported in this paper.

Funding: This research was funded by the University Grants Commission, Sanothimi, Bhaktapur, Nepal, as partial grants for PhD under award No: 078/079, S&T-07 and INSA/DST/ISRF/2023/NEP/03.

Data Availability Statement: Suggested Data Availability Statements are available in the section "MDPI Research Data Policies" at https://www.mdpi.com/ethics.

Conflicts of Interest: The authors declare no conflicts of interest.

References

1. Alamry KA, Khan A, Aslam J, Hussein MA, Aslam R. Corrosion inhibition of mild steel in hydrochloric acid solution by the expired Ampicillin drug. Sci Rep [Internet]. 2023;13(1):1–15. Available from: https://doi.org/10.1038/s41598-023-33519-y
2. Tobsin T, Bangchit P, Sirikullertrat V, Sutthiruangwong S. Influence of Sodium Dodecyl Sulfate on Corrosion Behavior of 304 Stainless Steel. Thammasat Int J Sc Tech. 2010;15(3):40–6. https://ph02.tci-thaijo.org/index.php/SciTechAsia/article/view/41284
3. Nahlé A, Salim R, EL Hajjaji F, Ech-chihbi E, Titi A, Messali M, et al. Experimental and theoretical approach for novel imidazolium ionic liquids as Smart Corrosion inhibitors for mild steel in 1.0 M hydrochloric acid. Arab J Chem. 2022;15(8). https:// doi: 10.1016/j.arabjc.2022.103967.
4. Karki N, Neupane S, Gupta DK, Das AK, Singh S, Koju GM, et al. Berberine isolated from Mahonia nepalensis as an eco-friendly and thermally stable corrosion inhibitor for mild steel in acid medium. Arab J Chem [Internet]. 2021;14(12):103423. Available from: https://doi.org/10.1016/j.arabjc.2021.103423
5. Jafari H, Akbarzade K, Danaee I. Corrosion inhibition of carbon steel immersed in a 1 M HCl solution using benzothiazole derivatives. Arab J Chem [Internet]. 2019;12(7):1387–94. Available from: https://doi.org/10.1016/j.arabjc.2014.11.018

6. Arun A, Rajkumar K, Sasidharan S, Balasubramaniyan C. Process parameters optimization in machining of monel 400 alloy using abrasive water jet machining. Mater Today Proc [Internet]. 2023;98(August 2023):28–32. Available from: https://doi.org/10.1016/j.matpr.2023.08.308
7. Singh A, Singh VK, Quraishi MA. Aqueous extract of kalmegh (andrographis paniculata) leaves as green inhibitor for mild steel in hydrochloric acid solution. Int J Corros. 2010;2010. https://doi: 10.1155/2010/275983.
8. Elkacimi Y, Achnin M, Aouine Y, Touhami ME, Alami A, Touir R, et al. Inhibition of mild steel corrosion by some phenyltetrazole substituted compounds in hydrochloric acid. Port Electrochim Acta. 2011;30(1):53–65. https:// doi: 10.4152/pea.201201053.
9. Malik MA, Hashim MA, Nabi F, AL-Thabaiti SA, Khan Z. Anti-corrosion ability of surfactants: A review. Int J Electrochem Sci. 2011;6(6):1927–48. https://doi.org/10.1016/S1452-3981(23)18157-0
10. Bae K, Kang M, Shin Y, Choi E, Kim Y. Multifunctional Edible Oil-Impregnated Nanoporous Oxide Layer on AISI 304 Stainless Steel. 2023; https://doi.org/10.3390/nano13050807
11. Du H, Wen J, Song G, Wu H. Corrosion Behavior of Ni / NiCr / NiCrAlSi Composite Coating on Copper for Application as a Heat Exchanger in Sea Water. 2023; https://doi.org/10.3390/nano13243129
12. Park K, Chang BY, Hwang S. Correlation between Tafel Analysis and Electrochemical Impedance Spectroscopy by Prediction of Amperometric Response from EIS. ACS Omega. 2019;4(21):19307–13. https://doi.org/10.1021/acsomega.9b02672
13. Hamid ZA, Soror TY, El-Dahan HA, Omar AMA. New cationic surfactant as corrosion inhibitor for mild steel in hydrochloric acid solutions. Anti-Corrosion Methods Mater. 1998;45(5):306–11. https://doi.org/10.1108/00035599810234605
14. Fateh A, Aliofkhazraei M, Rezvanian AR. Review of corrosive environments for copper and its corrosion inhibitors. Arab J Chem [Internet]. 2020;13(1):481–544. Available from: https://doi.org/10.1016/j.arabjc.2017.05.021
15. Migahed MA, Al-Sabagh AM. Beneficial role of surfactants as corrosion inhibitors in petroleum industry: A review article. Chem Eng Commun. 2009;196(9):1054–75. https://doi.org/10.1080/00986440902897095
16. Gupta DK, Awasthi L, Das AK, Yadav B, Ghimire A, Yadav AP. Corrosion Inhibition Effect of Acidic Extract of Bark of Eucalyptus Globulus on Mild Steel. Tribhuvan Univ J. 2020;35(1):1–10. https://doi.org/10.3126/tuj.v35i1.35828
17. Mobin M, Parveen M, Rafiquee MZA. Synergistic effect of sodium dodecyl sulfate and cetyltrimethyl ammonium bromide on the corrosion inhibition behavior of L-methionine on mild steel in acidic medium. Arab J Chem. 2017;10(July):S1364–72. https://doi.org/10.1016/j.arabjc.2013.04.006
18. Bammou L, Belkhaouda M, Salghi R, Benali O, Zarrouk A, Zarrok H, et al. Corrosion inhibition of steel in sulfuric acidic solution by the Chenopodium Ambrosioides extracts. J Assoc Arab Univ Basic Appl Sci [Internet]. 2014;16:83–90. Available from: http://dx.doi.org/10.1016/j.jaubas.2013.11.001
19. Karki N, Neupane S, Chaudhary Y, Gupta DK, Yadav AP. Berberis aristata: A highly efficient and thermally stable green corrosion inhibitor for mild steel in acidic medium. Anal Bioanal Electrochem. 2020;12(7):970–88.
20. Bashir S, Singh G. Shatavari (Asparagus Racemosus) as Green Corrosion Inhibitor of Aluminium in Acidic Medium. 2019;37(2):83–91. doi: 10.4152/pea.201902083.
21. Gorker L, Dimitrov V. Modified tafel equation for electroless metal deposition. Prog React Kinet Mech. 2009;34(2):127–40.
22. Yıldız R, Arslanhan S, Döner A, Baran MF. Corrosion behavior of mild steel in 1 M HCl with Cyclotrichium niveum as a green inhibitor. Mater Chem Phys. 2024;312(November 2023):1–17. doi: 10.1016/j.matchemphys.2023.128654. doi: 10.1108/PRT-03-2018-0020.
23. Tucker IM, Burley A, Petkova RE, Hosking SL, Thomas RK, Penfold J, et al. Surfactant/biosurfactant mixing: Adsorption of saponin/nonionic surfactant mixtures at the air-water interface. J Colloid Interface Sci. 2020;574:385–92.
24. Ikeuba A. Green corrosion protection for mild steel in acidic media : saponins and crude extracts of Gongronema latifolium Pigment & Resin Technology Article information : 2018;(August).
25. Khadke P, Tichter T, Boettcher T, Muench F, Ensinger W, Roth C. A simple and effective method for the accurate extraction of kinetic parameters using differential Tafel plots. Sci Rep [Internet]. 2021;11(1):8974. Available from: https://doi.org/10.1038/s41598-021-87951-z
26. Yuningsih CR, Trihanondo D, Kusnadi J, Utami AK. Corrosion Inhibition Efficiency of Tamarindus Indica Leaves Extracts on Mild Steel in Hydrochloric Acid Corrosion Inhibition Efficiency of Terminalia Catappa Leaves Extracts on Stainless Steel in Hydrochloric Acid. https://doi: 10.1088/1742-6596/1378/2/022051.
27. Y. Musa A, H. kadhum AA, Takriff MS, Daud AR, Kamarudin SK. Investigation on Ethylenediaminetetra-Acetic Acid as Corrosion Inhibitor for Mild Steel in 1.0M Hydrochloric Acid. Mod Appl Sci. 2009;3(4). https:// doi: 10.5539/mas.v3n4p90.

28. Arrousse N, Fernine Y, Al-Zaqri N, Boshaala A, Ech-Chihbi E, Salim R, et al. Thiophene derivatives as corrosion inhibitors for 2024-T3 aluminum alloy in hydrochloric acid medium. RSC Adv. 2022;12(17):10321–35. https://doi: 10.1039/d2ra00185c.
29. Mirzaee E, Sartaj M. The application of surfactant-enhanced soil washing process combined with adsorption using a recoverable magnetic granular activated carbon for remediation of PAH-contaminated soil. Environ Adv [Internet]. 2022;9(April):100274. Available from: https://doi.org/10.1016/j.envadv.2022.100274
30. Oyewole O, Oshin TA, Atotuoma BO. Corchorus olitorius stem as corrosion inhibitor on mild steel in sulphuric acid. Heliyon [Internet]. 2021;7(4):e06840. Available from: https://doi.org/10.1016/j.heliyon.2021.e06840
31. Deef Allah M, Abdelhamed S, Soliman KA, El-Etre MA. The performance of three novel Gemini surfactants as inhibitors for acid steel corrosion: experimental and theoretical studies. RSC Adv. 2021;11(59):37482–97. https:// doi: 10.1039/d1ra07449k.
32. Gnanam S, Rajendran V. Influence of Various Surfactants on Size, Morphology, and Optical Properties of CeO 2 Nanostructures via Facile Hydrothermal Route . J Nanoparticles. 2013;2013:1–6.
33. Shahi N, Kumar S, Singh S, Kumar C, Yadav B, Prasad A, et al. International Journal of Electrochemical Science Comparison of dodecyl trimethyl ammonium bromide (DTAB) and cetylpyridinium chloride (CPC) as corrosion inhibitors for mild steel in sulphuric acid solution. 2024;19(April). https://doi.org/10.1016/j.ijoes.2024.100575
34. Maiti K, Bhattacharya SC, Moulik SP, Panda AK. Physicochemistry of the binary interacting mixtures of cetylpyridinium chloride (CPC) and sodium dodecylsulfate (SDS) with special reference to the catanionic ion-pair (coacervate) behavior. Colloids Surfaces A Physicochem Eng Asp. 2010;355(1–3):88–98. https:// doi: 10.1016/j.colsurfa.2009.11.039.
35. Sethuraman MG, Raja PB. Corrosion inhibition of mild steel by Datura metel in acidic medium. Pigment Resin Technol. 2005;34(6):327–31. https:// doi: 10.1108/03699420510630345.
36. Mauro AC, Ribeiro BD, Garrett R, Borges RM, Da Silva TU, Paula Machado S De, et al. Ziziphus joazeiro stem bark extract as a green corrosion inhibitor for mild steel in acid medium. Processes. 2021;9(8):1–22. http:// doi: 10.3390/pr9081323..
37. Wang M, Du H, Guo A, Hao R, Hou Z. Microstructure control in ceramic foams via mixed cationic/anionic surfactant. Mater Lett [Internet]. 2012;88:97–100. Available from: http://dx.doi.org/10.1016/j.matlet.2012.08.028
38. Jia H, Lian P, Leng X, Han Y, Wang Q, Jia K, et al. Mechanism studies on the application of the mixed cationic/anionic surfactant systems to enhance oil recovery. Fuel [Internet]. 2019;258(August):116156. Available from: https://doi.org/10.1016/j.fuel.2019.116156
39. Goldraich M, Schwartz JR, Burns JL, Talmon Y. Microstructures formed in a mixed system of a cationic polymer and an anionic surfactant. Colloids Surfaces A Physicochem Eng Asp. 1997;125(2–3):231–44. http://doi: 10.1016/S0927-7757(96)03895-2.
40. Fayomi OSI, Popoola API, Oloruntoba T, Ayoola AA. Inhibitive characteristics of cetylpyridinium chloride and potassium chromate addition on type A513 mild steel in acid/chloride media. Cogent Eng. 2017;4(1):1–9. http://doi: 10.1080/23311916.2017.1318736.
41. Nallakukkala S. Comparative Study of Corrosion Inhibition in Carbon Steel Using Non-ionic Surfactants in Acidic Medium. Int J Chem Eng Process [Internet]. 2018;4(January):1. Available from: www.journalspub.com
42. Anderson AR. The Characteristics Of A True Leader. 2013;(January 2005). Available from: http://www.forbes.com/sites/amyanderson/2015/03/01/the-characteristics-of-a-true-leader/#470b00825bf7
43. Holland PM, Rubingh DN. Mixed Surfactant Systems. Fuel Sci Technol Int. 1993;11(1):241–2. http://doi: 10.1080/08843759308916065.
44. Ramezanzadeh M, Sanaei Z, Bahlakeh G, Ramezanzadeh B. Highly effective inhibition of mild steel corrosion in 3.5% NaCl solution by green Nettle leaves extract and synergistic effect of eco-friendly cerium nitrate additive: Experimental, MD simulation and QM investigations [Internet]. Vol. 256, Journal of Molecular Liquids. Elsevier B.V; 2018. 67–83 p. Available from: https://doi.org/10.1016/j.molliq.2018.02.021
45. Pon-On W, Meejoo S, Tang IM. Formation of hydroxyapatite crystallites using organic template of polyvinyl alcohol (PVA) and sodium dodecyl sulfate (SDS). Mater Chem Phys. 2008;112(2):453–60. http:// doi: 10.1016/j.matchemphys.2008.05.082. doi: 10.3126/jncs.v44i1.62690.
46. Yadav CK, Niraula TP, Neupane S, Yadav AP, Bhattarai A. Study of Anti-Corrosion Properties of Sodium Dodecyl Sulphate and Cetyl Pyridinium Chloride. J Nepal Chem Soc. 2024;44(1):163–72. http://doi: 10.3126/jncs.v44i1.62690.
47. Lone MS, Afzal S, Chat OA, Aswal VK, Dar AA. Temperature-and composition-induced multiarchitectural transitions in the catanionic system of a conventional surfactant and a surface-active ionic liquid. ACS Omega. 2021;6(18):11974–87. http://doi: 10.1021/acsomega.1c00469.

 doi:10.20944/preprints202404.1187.v2

48. Ghosh D, Bhattarai A, Das B. Electrical conductivity of sodium polystyrenesulfonate in acetonitrile - Water-mixed solvent media: Experiment and data analysis using the Manning counterion condensation model and the scaling theory approach. Colloid Polym Sci. 2009 Sep;287(9):1005–11. doi: 10.1007/s00396-009-2055-7.
49. Chemistry P. Micellar Characterisation of Saponin from Sapindus Mukorossi. 2006;43:262–8. https://doi.org/10.3139/113.100315
50. Ramírez Coutiño VA, Torres Bustillos LG, Godínez Mora Tovar LA, Guerra Sánchez RJ, Rodríguez Valadez FJ. pH effect on surfactant properties and supramolecular structure of humic substances obtained from sewage sludge composting. Rev Int Contam Ambient. 2013;29(3):191–9.
51. Sachin KM, Karpe S, Singh M, Bhattarai A. Physicochemical Properties of Dodecyltrimethylammonium Bromide (DTAB) and SodiumDodecyl Sulphate (SDS) Rich Surfactants in Aqueous Medium, At T = 293.15, 298.15, and 303.15 K. Macromol Symp. 2018 Jun 1;379(1). http:// doi: 10.1002/masy.201700034.
52. Belhaj AF, Elraies KA, Mahmood SM, Zulkifli NN, Akbari S, Hussien OSE. The effect of surfactant concentration, salinity, temperature, and pH on surfactant adsorption for chemical enhanced oil recovery: a review. J Pet Explor Prod Technol [Internet]. 2020;10(1):125–37. Available from: https://doi.org/10.1007/s13202-019-0685-y
53. Mondal BB, Banik R, Ghosh S. n Pr f. Colloids Surfaces A Physicochem Eng Asp [Internet]. 2023;132781. Available from: https://doi.org/10.1016/j.colsurfa.2023.132781
54. Kupsch S, Eggers LF, Spengler D, Gisch N, Goldmann T, Fehrenbach H, et al. Characterization of phospholipid-modified lung surfactant in vitro and in a neonatal ARDS model reveals anti-inflammatory potential and surfactant lipidome signatures. Eur J Pharm Sci [Internet]. 2022;175(December 2021):106216. Available from: https://doi.org/10.1016/j.ejps.2022.106216
55. Abdallah M, Soliman KA, Al-Gorair AS, Al Bahir A, Al-Fahemi JH, Motawea MS, et al. Enhancing the inhibition and adsorption performance of SABIC iron corrosion in sulfuric acid by expired vitamins. Experimental and computational approach. RSC Adv. 2021;11(28):17092–107. http://doi: 10.1039/d1ra01010g.
56. Pavelyev RS, Zaripova YF, Yarkovoi V V., Vinogradova SS, Razhabov S, Khayarov KR, et al. Performance of waterborne polyurethanes in inhibition of gas hydrate formation and corrosion: Influence of hydrophobic fragments. Molecules. 2020;25(23). http://doi: 10.3390/molecules25235664.
57. D'Souza R, Nithin TP, Sirisha N. Review of Action of Cationic and Anionic Surfactants on Corrosion Inhibition of Steel in Acidic Medium. Int J Adv Res Sci Eng. 2015;4(2):69–76. http://www.ijarse.com